Thermochimica Acta, 111 (1987) 103–113
Elsevier Science Publishers B.V., Amsterdam – Printed in The Netherlands

RELATED THERMAL ANALYSES AND SPECTROPHOTOMETRIC STUDIES ON IODINE REDOX PRODUCTS OF AMINOPHENOLS

M.A. ZAYED

Chemistry Department, Faculty of Science, University of Cairo, Giza (Egypt)

(Received 4 June 1986)

ABSTRACT

Three redox products obtained by oxidation of aminophenols with iodine in aqueous iodide have been isolated from the redox reaction medium. Characterization involves elemental, thermogravimetric and differential thermal analyses, IR, UV and visible spectrometry. Structural formulae of these redox products were suggested depending upon the results of these studies. The identification and characterization of these redox products confirm the previously proposed schemes representing these redox reactions.

INTRODUCTION

The separation and identification of radicals, intermediates and final redox products obtained by electro-oxidation, or by oxidation with inorganic oxidants, of aromatic reducing agents usually enable one to suggest the most probable mechanisms of these redox reactions [1–7]. Mohilner et al. [6] identified, using IR and elemental analysis, the anodic oxidation product of aniline as a precipitate known as emeraldien which had the structural formula

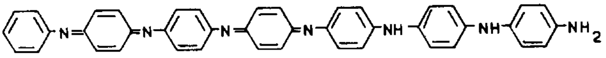

This product was formed by dimerization, followed by polymerization of the cation radicals obtained;

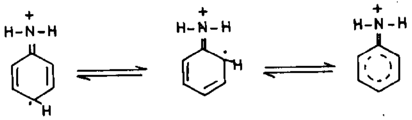

Oxidation of aminophenols with Ce(IV) salts [7] leads to the formation of quinoneimine cation radicals which either dimerized or polymerized by *o*-, *p*- or *m*-coupling to form nonidentified solid products.

The structure identification of the separated solid redox products obtained by oxidation of halogenated simple monohydric phenols with iodine

0040-6031/87/$03.50

was performed in our laboratory [2] by thermal analysis and spectrophotometric studies. The dimerization or polymerization of the cation radicals obtained was inhibited by iodination of these radicals to give the final redox products. Therefore, the products obtained are monomers of the general formula $X \cdot C_6H_4I_2O \cdot 2H_2O$. This study confirmed the previously proposed mechanism of these redox reactions [2,5].

Kinetic and potentiometric studies of the redox reactions between iodine and aminophenols were recently reported elsewhere [8,9]. In order to throw more light on the most probable mechanisms of these redox reactions, identification of structures of the redox products obtained was the ultimate aim of the present investigation using thermal and spectral measurements.

EXPERIMENTAL

Materials and solutions

The water used was always double-distilled in glass. The chemicals were all of the highest purity available.

The 0.05 M solution (6.39 g l^{-1}) in aqueous potassium iodide (10 g l^{-1}) was prepared and kept in a dark flask. Stock solutions of 0.025 M *o*-aminophenol (*o*-AP), *p*-aminophenol (*p*-AP) and *m*-aminophenol (*m*-AP) were prepared by dissolving the calculated accurate weights in the required volume of double distilled water. The 0.05 M sodium hydroxide solution was prepared from the carbonate-free stock solution. This solution was used to adjust the pH of the redox reaction medium to pH 8–10 using a pH/mV meter Orion Research Model 701 A digital Ionlyzer with combined pH electrode Orion Model 91-02.

Preparation of the solid redox products

75 ml of iodine solution was added to 50 ml of aminophenol with constant stirring for complete mixing and the pH of the solution adjusted by gradual addition of aqueous sodium hydroxide solution, until the solid redox product just appeared at pH 8–10; at pH > 10 the precipitate obtained may dissolve. The solid product coagulated rapidly within 5 min on gentle warming on a water bath. The precipitate from the motherliquor was then filtered through a porcelain Buchner funnel using a water pump and the precipitate washed several times with hot distilled water. The dried solid redox products were crystallized twice from an ethanol–water mixture. The reddish-violet solid product of *o*-AP has a m.p. of 240°C, whereas the deep violet redox product of *p*-AP has a m.p. of 250°C and the brown product of *m*-AP has a m.p. of 138 ± 1°C.

The same solid products were also obtained from the redox reaction medium in a potentiometric follow-up of these redox reactions [9].

TABLE 1

Elemental analysis of aminophenol–iodine redox products

Compound [a]	Found (%)					Calc. (%)				
	C	H	N	I	M.W.	C	H	N	I	M.W.
I	51.8	4.0	10.1	23.9	560	51.98	3.42	10.10	22.9	554
II	38.4	2.8	6.4	51.9	770	37.84	2.75	5.52	50.1	764
III	18.2	1.35	4.10	71.5	725	19.05	1.58	3.70	67.2	720

[a] The suggested formulae of the redox products of aminophenols due to elemental analysis are: **I**, $C_{24}H_{19}IN_4O_4$; **II**, $C_{24}H_{21}I_2N_3O_2$; **III**, $C_{12}H_8I_4O_2$.

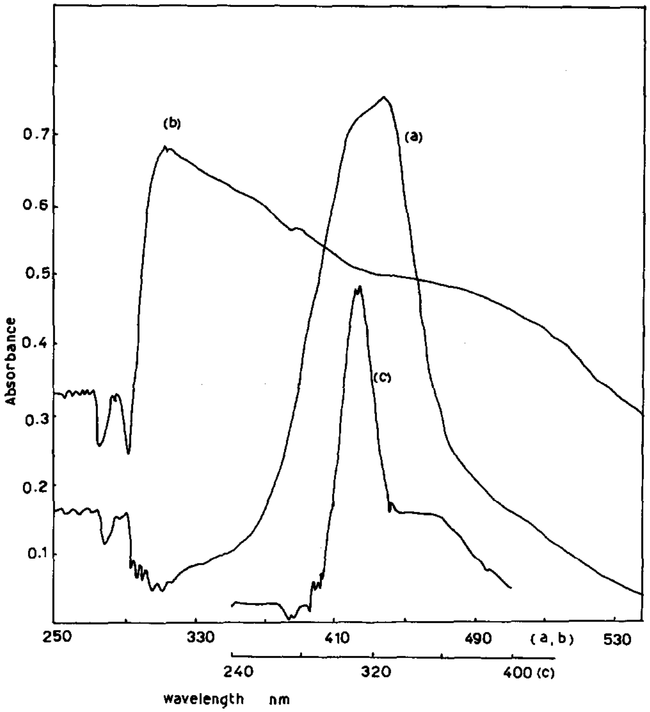

Fig. 1. Absorption spectra of iodine-aminophenols oxidation products: (a) *o*-AP; (b) *p*-AP; (c) *m*-AP.

Elemental microanalysis (Table 1) of the redox products for C, H, N, I and M.W. determinations were performed in the microanalytical center at Cairo University.

Spectrophotometric measurements

The absorption spectra (Fig. 1) of *o*-AP and *p*-AP redox products in their ethanolic solutions (10 mg/50 ml EtOH) were measured at 250–600 nm and that of *m*-AP solution (30 mg/50 ml EtOH) was measured at 240–400 nm using a PYE UNICAM SP 1750 recording spectrophotometer.

The IR of all the solid products (Fig. 2) were recorded in the region 250–4000 cm^{-1} using Beckman IR Spectrophotometer 1180 (Fulletron, CA, U.S.A.) applying the potassium bromide disc technique.

Thermal analysis of the redox products (TGA and DTA)

Thermogravimetric analysis (TGA) and differential thermal analysis (DTA) were done using a conventional thermal analyzer (Shimadzu System-Shimadzu 30 series thermal analysis instrument). The weight losses (from 2.5

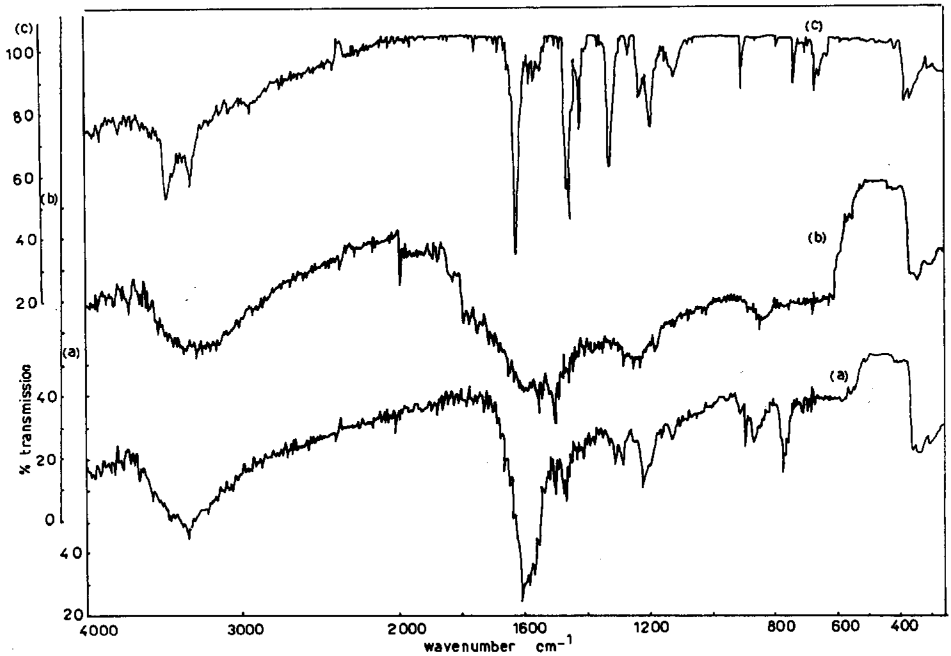

Fig. 2. IR of iodine-aminophenols oxidation products: (a) *o*-AP; (b) *p*-AP; (c) *m*-AP.

mg sample) and heat response of the changes in the sample were measured from room temperature to 480, 360 and 280 °C for *o*-AP, *p*-AP and *m*-AP redox products respectively (Fig. 3). The DTA (Fig. 4) was performed in the temperature range from room temperature to 280 °C for both *p*-AP (as an example of polymeric forms) and the *m*-AP redox products. The heating rate

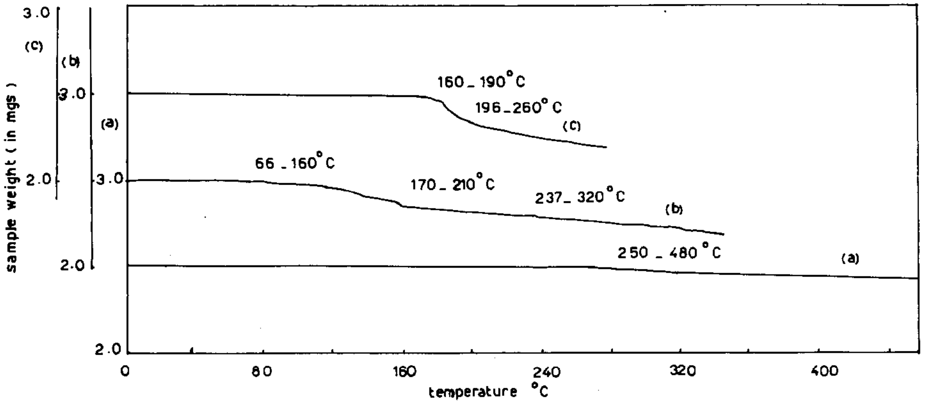

Fig. 3. TGA of iodine aminophenol redox products: (a) *o*-AP; (b) *p*-AP and (c) *m*-AP.

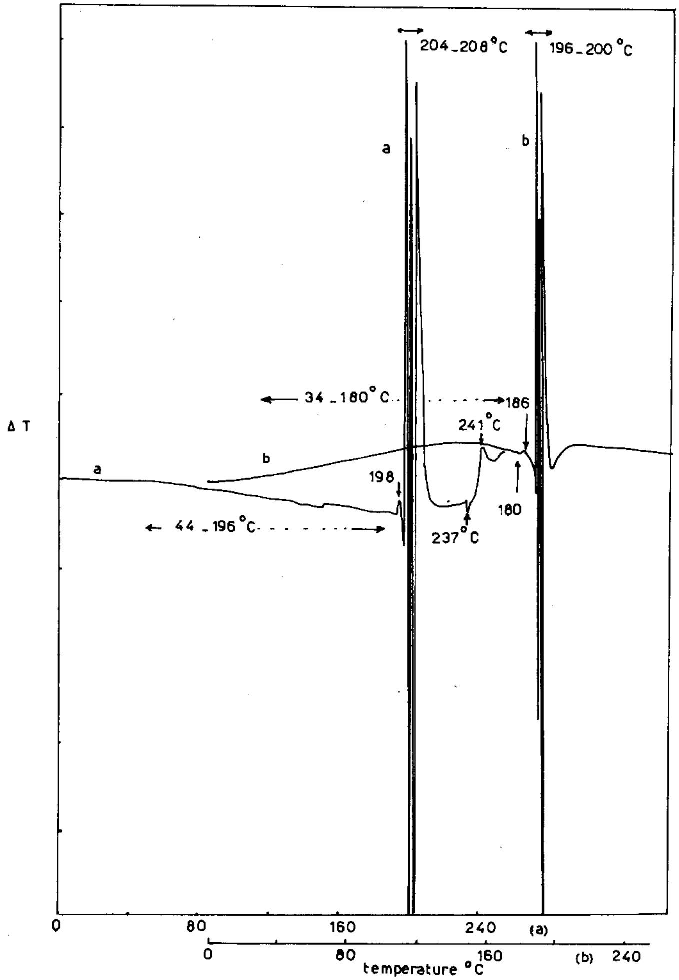

Fig. 4. DTA of iodine aminophenol redox products: (a) *p*-AP and (b) *m*-AP.

was 10°C min^{-1} in both TGA and DTA. The thermal analyses were performed at the Center of Radiation Technology in El-Nasr City, Cairo.

RESULTS AND DISCUSSION

From the microanalysis data presented in Table 1 of the separated solid products for elements C, H, N, I and the M.W., the suggested formulae are $C_{24}H_{19}IN_4O_4$, $C_{24}H_{21}I_2N_3O_2$ and $C_{12}H_8I_4N_2O_2$ for the redox products of *o*-AP, *p*-AP and *m*-AP, respectively.

Kinetic studies [8] of the redox reactions between iodine and aminophenol reductants, as previously made in our laboratory, indicated the formation of the solid redox products by polymerization of the quinoneimine cation radicals obtained in the case of *o*-AP and *p*-AP and their dimerization in the case of *m*-AP. The proposed structure of the polymer cation radical was $^{+}O{-}C_6H_4{-}N{=}C_6H_4{-}N{=}C_6H_4{-}N{=}C_6H_4{-}O^{+}$ symbolized as (*o*- or *p*-QI)$_4^{2+}$ in the oxidation of *o*- or *p*-APs and $^{+}O{-}C_6H_4NH \cdot NH \cdot C_6H_4{-}O^{+}$ as a dimer of symbol (*m*-QI)$_2^{2+}$ in the case of the *m*-substituent. Iodination of the polymeric or dimeric cation radicals obtained was proposed to inhibit further polymerization of these radicals by formation of the solid redox products under investigation.

Based on the microanalysis and kinetic data, together with the idea of polymerization of aniline cation radicals given by Mohilner [6], the possible structural formulae of the solid products under investigation may be represented by **I**, **II** and **III** for *o*-, *p*- and *m*-substituents respectively.

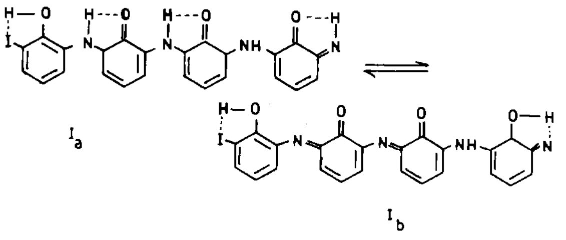

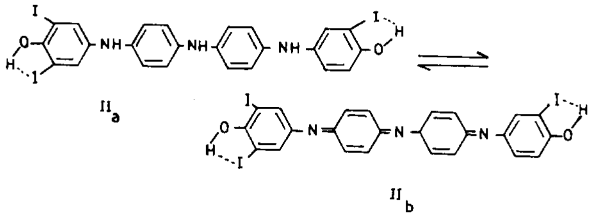

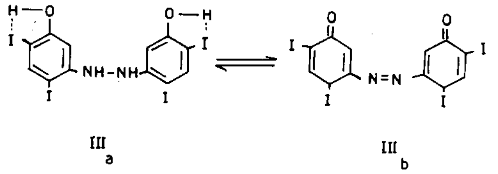

The presence of a strong band at 442 nm in Fig. 1a (ϵ; 2.09×10^4), which may be due to the π–π^* transitions of the delocalized π-electrons in a hybrid of the canonical structure **Ia** and **Ib**, confirms the conjugation in this compound. The smaller band at 286 nm (ϵ; 4.17×10^3) may be attributed to the π–π^* transitions in the quinone form **Ib**. The less significant bands (ϵ; $\simeq 1900$) in the range 290–320 nm reasonably refer to n–π^* transitions by the non-bonding electrons of the weakly hydrogen bonded oxygen, nitrogen or halogen atoms [10] in the given compound.

In case of the *p*-AP product, the spectra (Fig. 1b) show a small band at 284 nm (ϵ; 1.2×10^4) which interprets the π–π^* transitions within the less dominant form **IIb**. It is noticed that n–π^* transitions are absent which indicates that almost all the heterogenous atoms (O, N and I) are not free but are rather strongly bonded as in structures **II**. The other bands at 318 nm (ϵ; 2.62×10^4), at 390 nm (ϵ; 2.12×10^4) and the intense shoulder at 410–530 nm may be attributed to the π–π^* transitions of the delocalized π-electrons in the highly conjugated structure **IIb**.

The spectra of the solid redox product of *m*-AP (Fig. 1c) refer to the presence of very small peaks in the range of 260–290 nm ($\epsilon \simeq 10^2$) which are assigned as n–π^* transitions due to nonbonding electrons of halogen, nitrogen and oxygen atoms in the hybrid form of cannonical structures **III**. The intense band centered at 308 nm (ϵ; 0.55×10^4) represents π–π^* transitions of the π-electrons in the hydrazone group in structure **IIIa** [11,12]. The other smaller bands at 330 nm (ϵ; 1.83×10^3) and at 384 nm (ϵ; 0.96×10^3) are assigned as π–π^* transitions of the delocalized π-electrons in the given ring system of compound **III**. The band at 286 nm (ϵ; 6.26×10^2) may be attributed to π–π^* transitions in the azo structure **IIIb** which is expected to be less dominant than **IIIa**.

The IR spectra of the solid products, **I**, **II** and **III** are shown in Fig. 2. The IR bands at 330–350 and 650–670 cm^{-1} represent different C–I modes of vibrations [13]. The frequencies in the range 880–900 cm^{-1} are identified as the aryl C–N modes, whereas the bands at 1340–1350 cm^{-1} and 1550–1650 cm^{-1} are attributed to the secondary aromatic amines. The bands at 1100, 1170, 1200 and 1250–1270 cm^{-1} refer to different modes of C–O phenolic and OH groups. The frequencies at 1450–1550 cm^{-1} are usually assigned to the ring system vibrations. The bands in the range 1700–1740 cm^{-1} refer mostly to conjugated carbonyl groups in 5- or 6-membered aryl rings. Finally the intense bands in the IR spectra of the polymeric oxidation products of *o*-AP and *p*-AP at 3200–3600 cm^{-1} in the case of **I** and at 3000–3600 cm^{-1} in the case of **II** or that at 3250 and 3450 cm^{-1} in the case of **III** are attributed to intramolecular and weakly bonded OH interactions in these compounds [14].

From the above discussion it is clear that UV, visible and IR spectra support the proposed structural formulae of the redox products obtained from aminophenols and find great accordance with the elemental analysis.

Thermal analysis TGA and DTA

Thermal analysis involves very useful techniques for studying the thermal decomposition of solid substances involving simple [2] and complex compounds [15,16]. Further details about the use of thermal analysis have been reported elsewhere [17,18] and skilful manipulation of these techniques was reported recently [2,15,16].

Figure 3 illustrates TGA curves for compounds **I**, **II** and **III** respectively within a temperature ranging from room temperature up to 480°C. The estimated mass losses were computed based on TGA and the calculated mass losses were computed using the results of microanalysis (Table 1).

For TGA of the thermally stable *o*-AP redox product **I** (Fig. 3a) the single estimated mass loss is 4.15% which accounts reasonably for the loss of two nitrogen atoms together with the liberation of two hydrogen atoms after fragmentation of the polymer **I** (calc. wt. loss 4.0%). This occurs in the temperature range 250–480°C.

The TGA curve of the *p*-AP redox polymer product **II** (Fig. 3b) gives the first estimated mass loss of 6.0% within the temperature range 66–180°C which may be due to liberation of N_2 and NH_3 molecules (calc. wt. loss 5.88%) [18]. The second estimated mass loss (4.0%) at 170–210°C and the third mass loss (4.0%) at 237–320°C account reasonably for the successive mass losses of one CO group in each step (calc. wt. loss 3.66%) obtained by fragmentation of the molecular phenols or quinones resulting from the decomposition of the less stable polymer **II**, in a manner similar to the mass spectra of phenol [19]

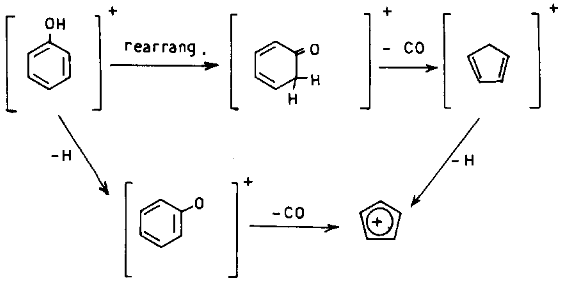

On the other hand the TGA curve for the *m*-AP redox product **III** (Fig. 3c) exhibiting the first estimated mass loss (4.0%) within the temperature range 160–190°C might be attributed to the loss of N_2 gas together with three H atoms (calc. wt. loss 4.44%). This indicates fragmentation of the given canonical structure **III** in this temperature range. The second estimated mass loss (8.0%) within the temperature range 196–260°C is accounted for by the loss of two CO groups from the decomposed fragments of the dimer **III** (calc. wt. loss 8.33%) [19].

DTA curves for redox product of *p*-AP **II**, representing the polymers **I** and **II**, and of dimer **III** of *m*-AP are graphically represented in Fig. 4. Curve (a) indicates the appearance of a broader endotherm starting from 44 to 150°C followed by another broad one at 152–196°C. A weak exotherm appears at about 198°C. This is followed by a series of very strong exotherms and endotherms very close to each other within a small temperature range 204–208°C, a weak endotherm at 237°C and finally a similar exotherm at 241°C.

The appearance of the broader endotherms in the temperature range 44–196°C might be related to the decomposition of N_2 and NH_3 molecules from the moiety of the decomposed polymer **II** as confirmed by a TGA mass loss at approximately the same temperature range (66–166°C). The weak exotherm at 198°C may indicate an interaction between one of the decomposed nitrogen atoms and the liberated hydrogen atoms to form a gaseous ammonia molecule. The appearance of the very strong exotherms and endotherms at 204–208°C may be attributed to the vigorous decomposition of a CO group followed by its vigorous oxidation to CO_2 at this temperature range. This is also confirmed by the mass loss indicated in TGA at 170–210°C. The appearance of a finite sharp endotherm at 237°C may be due to the less vigorous decomposition of another CO group which is oxidized at 241°C as confirmed by the appearance of an exotherm at this temperature. This is also confirmed by the successive mass loss at 237–320°C of the second CO group in TGA.

The DTA curve (Fig. 4b) of the *m*-AP redox product **III** shows a broader exotherm within the temperature range 34–180°C which may indicate secondary interactions of the sample with environment moisture and might be subjected to some aggregation effects for the sample multiples or particulates. A finite endotherm appears at 180°C which may be attributed to the decomposition of the dimer **III** to given nitrogen and hydrogen atoms. This is confirmed by the mass loss given in TGA at the same temperature range 160–190°C. The small exotherm appearing at 186°C is assumed to be due to the interaction of nitrogen and hydrogen atoms to form a NH_3 gas molecule which is a result of the above decomposition. The appearance of successive strong endotherms and exotherms within the temperature range 196–198°C is attributed to the successive decomposition of CO groups and their spontaneous oxidation into CO_2 at this temperature range. This is confirmed by TGA mass losses of two CO groups at 196–260°C.

ACKNOWLEDGEMENT

Thanks are due to Dr. F.A. Nour El-Dien, lecturer of analytical chemistry, Faculty of Science, University of Cairo, for her help throughout the whole work.

REFERENCES

1 R.N. Adams, Electrochemistry at Solid Electrodes, Chap. 10, Marcel Dekker, Inc., New York, 1969.

2 M.A. Zayed, Can. J. Chem., 1986, submitted.
3 E. Adler et al., Acta Chem. Scand., 25(6) (1971) 2055–2069; 25(7) (1971) 2775-2776; 29(9) (1975) 909-920.
4 D.N. Sharma, Ind. Chem., 11 (1973) 756.
5 M.A. Zayed, H. Khalifa and E.A. Nour El-Dien, Thermochim. Acta, 101 (1986) 325.
6 D.M. Mohilner, R.N. Adams and Argersinger, J. Am. Chem. Soc., 84 (1962) 3618.
7 I. Bacon and R.N. Adams, J. Am. Chem. Soc., 90 (1968).
8 M.A. Zayed, J. Am. Chem. Soc., submitted.
9 H. Khalifa, M.A. Zayed and F.A. Nour El-Dien, Egypt. J. Chem., 27 (1984) 747.
10 N.M. Kayrayannis, J.T. Caronin, C.M.M. Kulski, L.L. Pytlewski and M.M. Lages, J. Inorg. Nucl. Chem., 33 (1971) 4334.
11 Y. Yagi, Bull. Chem. Soc. Jpn., 36 (1963) 487, 492.
12 H.C. Yao, J. Org. Chem., 29 (1964) 2959.
13 B.S. Furniss, A.J. Hannaford, V. Rogers, P.W.G. Smith and A.R. Tatchell, Vogel Text Book of Practical Organic Chemistry, 4th edn., Longman, London, 1980, pp. 1271–1282.
14 D.H. Williams and I. Fleming, Spectrophotometric Methods in Organic Chemistry, McGraw-Hill, London, 1966, p. 54.
15 M.A. Zayed, M.M. Khater, M.S. Rizk, H.M. Abd El-Fattah and A.M. Khalil, Thermochim. Acta, 87 (1983) 125.
16 M.A. Zayed, M.M. Khater, M.S. Rizk and H.M. Abd El-Fattah, Thermochim. Acta, 73 (1984) 217.
17 D. Dolimore, in R.C. Mackenzie (Ed.), Differential Thermal Analysis, Vol. 1, Academic Press, London, 1970, Chap. 13.
18 H.H. Willard, L.L. Merritt and J.A. Dean, Instrumental Methods of Analysis, 5th edn., Affiliated East-West Press PVT Ltd., New Delhi, Madras, 1977, pp. 794–521.
19 I.L. Finar, Organic Chemistry, Vol. 1, Low-Priced edn., Toppon, Singapor, 1985, p. 700.